Impaired Integrin-mediated Adhesion and Signaling in Fibroblasts Expressing a Dominant-negative Mutant PTP1B

Carlos O. Arregui, Janne Balsamo, and Jack Lilien

Department of Biological Sciences, Wayne State University, Detroit, Michigan 48202

Abstract. To investigate the role of nonreceptor protein tyrosine phosphatase 1B (PTP1B) in β1-integrin–mediated adhesion and signaling, we transfected mouse L cells with normal and catalytically inactive forms of the phosphatase. Parental cells and cells expressing the wild-type or mutant PTP1B were assayed for (*a*) adhesion, (*b*) spreading, (*c*) presence of focal adhesions and stress fibers, and (*d*) tyrosine phosphorylation. Parental cells and cells expressing wild-type PTP1B show similar morphology, are able to attach and spread on fibronectin, and form focal adhesions and stress fibers. In contrast, cells expressing the inactive PTP1B have a spindle-shaped morphology, reduced adhesion and spreading on fibronectin, and almost a complete absence of focal adhesions and stress fibers. Attachment to fibronectin induces tyrosine phosphorylation of focal adhesion kinase (FAK) and paxillin in parental cells and cells transfected with the wild-type PTP1B, while in cells transfected with the mutant PTP1B, such induction is not observed. Additionally, in cells expressing the mutant PTP1B, tyrosine phosphorylation of Src is enhanced and activity is reduced. Lysophosphatidic acid temporarily reverses the effects of the mutant PTP1B, suggesting the existence of a signaling pathway triggering focal adhesion assembly that bypasses the need for active PTP1B. PTP1B coimmunoprecipitates with β1-integrin from nonionic detergent extracts and colocalizes with vinculin and the ends of actin stress fibers in focal adhesions. Our data suggest that PTP1B is a critical regulatory component of integrin signaling pathways, which is essential for adhesion, spreading, and formation of focal adhesions.

Key words: protein tyrosine phosphatase • integrins • cell-substrate adhesion • cell signaling • tyrosine phosphorylation

Aɴ increasing body of evidence indicates that the function of adhesion receptors is controlled by signaling pathways regulating their association with the cytoskeleton (for reviews see Luna and Hitt, 1992; Gumbiner, 1993; Lilien et al., 1997; Yamada and Geiger, 1997). A major feature of these signaling pathways is tyrosine phosphorylation/dephosphorylation of proteins that link or modulate the interaction of adhesion receptors with the actin-containing cytoskeleton. Among cadherins, this linkage is mediated by α- and β- or γ-catenin (for reviews see Kemler, 1993; Aberle et al., 1996). Hyperphosphorylation of β-catenin on tyrosine residues is correlated with the loss of cadherin function (Behrens et al., 1993; Hamaguchi et al., 1993; Balsamo et al., 1996; Daniel and Reynolds, 1997; Hazan and Norton, 1998; Ozawa and Kemler, 1998) and destabilization or loss of the actin–cadherin linkage (Balsamo et al., 1996; Fujii et al., 1996; Daniel and Reynolds,

1997; Hazan and Norton, 1998; Ozawa and Kemler, 1998). Our laboratory has shown that, in retinal cells, dephosphorylation of β-catenin by the nonreceptor protein tyrosine phosphatase PTP1B is essential for N-cadherin function (Balsamo et al., 1996). Moreover, in fibroblasts constitutively expressing N-cadherin that are transfected with a dominant-negative mutant PTP1B, β-catenin retains phosphate on tyrosine residues, N-cadherin is uncoupled from the cytoskeleton, and N-cadherin–mediated adhesion is lost (Balsamo et al., 1998).

Tyrosine phosphorylation/dephosphorylation is also critical to integrin-mediated adhesion and focal contact formation (for reviews see Clark and Brugge, 1995; Schwartz et al., 1995; Jockusch et al., 1995; Parsons, 1996; Yamada, 1997). Vinculin, talin, and α-actinin, which are prominent structural components of focal contacts, mediate the anchorage of actin stress fibers at these sites (for reviews see Burridge et al., 1988; Jockusch et al., 1995; Burridge and Chrzanowska-Wodnicka, 1996). Other proteins of focal adhesions, such as paxillin and p130Cas, appear to function as adaptors, while focal adhesion kinase

---

Address all correspondence to Jack Lilien, Department of Biological Sciences, Wayne State University, Detroit, MI 48202. Tel.: (313) 577-2783. Fax: (313) 577-6891. E-mail: jlilien@biology.biosci.wayne.edu

(FAK)[1] and Src, among others, are important intracellular signaling components (for reviews see Jockusch et al., 1995; Schwartz et al., 1995; Burridge and Chrzanowska-Wodnicka, 1996). Recent mutational studies have outlined a sequence of tyrosine phosphorylation events after integrin engagement. Early in this sequence, tyrosine 397 on FAK is autophosphorylated, creating a high-affinity binding site for the SH2 domain of the Src family kinases, recruiting Src and/or Fyn into integrin complexes (Lipfert et al., 1992; Schaller et al., 1994; Xing et al., 1994; Eide et al., 1995). Recruitment and activation of Src leads to phosphorylation of FAK on additional tyrosine residues, contributing to its full activation and to the recruitment of additional proteins to integrin complexes (Calalb et al., 1995; Brown and Cooper, 1996; Hanks and Polte, 1997; Parsons and Parsons, 1997). The formation of this complex appears to be important for tyrosine phosphorylation of downstream targets, including paxillin (Schaller and Parsons, 1995). A late manifestation of this chain of tyrosine phosphorylations, in which FAK and Src are primary actors, is the assembly of focal adhesions. Consistent with a role for tyrosine kinases in focal contact assembly, the tyrosine kinase inhibitor herbimicin A inhibits the phosphorylation of FAK and paxillin and the formation of focal adhesions and stress fibers among fibroblasts plated on fibronectin (Burridge et al., 1992). The balance between tyrosine phosphorylation and dephosphorylation appears to be critical to the normal assembly of focal adhesions. Expression of v-Src (Rohrschneider, 1980; Nigg et al., 1982; Krueger et al., 1983; Nermut et al., 1991) or deregulated c-Src (Howel and Cooper, 1994; Thomas et al., 1995) leads to hyperphosphorylation of focal adhesion components, aberrant formation of focal adhesion sites, and alteration of the actin cytoskeleton.

While tyrosine kinases have been a major focus of attention in the analysis of focal adhesion formation and in the tyrosine phosphorylation occurring after integrin–matrix interaction, a potential role for tyrosine phosphatases in focal adhesion assembly is beginning to emerge. Several lines of evidence suggest that PTP1B may play a role. Engagement of integrins in platelets and T lymphocytes is accompanied by cleavage of PTP1B from a 50- to a 42-kD form and by its translocation to the cytoskeleton (Frangioni et al., 1993; Ezumi et al., 1995; Rock et al., 1997). Both the full-length and the proteolytically processed forms of PTP1B associate with and dephosphorylate p130Cas, an adaptor molecule found in focal adhesion complexes (Liu et al., 1996; Rock et al., 1997). A proline-rich region near the COOH terminus of PTP1B is essential for association with the Src-homology 3 domain of p130Cas (Liu et al., 1996, 1998).

In the present work we report that the expression of a catalytically inactive PTP1B, but not the wild-type, blocks integrin-mediated cell adhesion and spreading. We also present evidence indicating that PTP1B associates with integrin-containing complexes in focal adhesions. Furthermore, the catalytically inactive form of PTP1B blocks the fibronectin-induced tyrosine phosphorylation of FAK and paxillin, suggesting that PTP1B plays a role in regulating the function of critical tyrosine kinases such as Src and FAK. We discuss potential mechanisms through which PTP1B may affect this signaling pathway.

Materials and Methods

Materials

DiI and rhodamine B hexyl ester were from Molecular Probes (Eugene, OR); fetal bovine serum and peptides were from GIBCO BRL (Grand Island, NY); bovine plasma fibronectin was from Calbiochem (San Diego, CA); sodium vanadate ($NaVO_3$), leupeptin, and PMSF were from Sigma Chemical Co. (St. Louis, MO). Bovine serum albumin (fraction V), molecular biology grade, was from Fisher Scientific (Pittsburgh, PA).

Antibodies

Monoclonal antibodies against FAK (clone 77) and paxillin (clone 349) were from Transduction Laboratories (Lexington, KY). Monoclonal antibody against mouse β1-integrin (clone MB1.2) was from Chemicon International (Temecula, CA), and a polyclonal anti–β1-integrin was a generous gift of Dr. Ruoslahti (The Burnham Institute, La Jolla, CA). Monoclonal antiphosphotyrosine antibody (clone 4G10) and polyclonal anti-PTP1B antibody were from Upstate Biotechnology, Inc. (Lake Placid, NY), and the monoclonal anti–human vinculin (clone hVIN-1) and phalloidin–TRITC were from Sigma Chemical Co. Polyclonal, anti-cSrc antibody was from Santa Cruz Biotechnology (Santa Cruz, CA). Peroxidase-conjugated goat anti–mouse IgG and FITC-conjugated goat anti–rat IgG were from Cappel (Organon Teknika Corp., Durham, NC). Peroxidase-conjugated donkey anti–rabbit IgG, FITC-conjugated donkey anti–mouse IgG, and FITC-conjugated donkey anti–rabbit IgG were from Jackson ImmunoResearch Laboratories (West Grove, PA). The polyclonal anti-GFP antibody was from CLONTECH Laboratories (Palo Alto, CA).

Cell Culture and Transfection

Mouse L cell fibroblasts were cultured in DME (GIBCO BRL) supplemented with 5% fetal bovine serum. Stable transfectants expressing the wild-type chick PTP1B or an inactive form with a mutation in the active site (C215S) were prepared as described (Balsamo et al., 1998). In brief, catalytically inactive (C215S) PTP1B was created by site-directed mutagenesis and recombinant PCR. A c-myc tag was added in frame to the 5′ end of both the wild-type and mutant PTP1B cDNA, and the constructs were cloned into the eukaryotic vector pcDNA3.1/zeo (Invitrogen, Carlsbad, CA) and delivered to cells using Lipofectin (GIBCO BRL). Transfected cells were selected by culturing in the presence of 500 μg/ml zeocin (Invitrogen). Individual clones were selected and expanded for analysis, and multiple aliquots were frozen. To avoid potential changes in each cell line, each aliquot of frozen cells was used for no more than 2 wk.

Green fluorescent protein (GFP)-tagged PTP1B was prepared using the pEGFP-C3 vector (CLONTECH Laboratories). Wild-type and C215S mutant chick PTP1B cDNAs were amplified by PCR using primers that create restriction enzymes sites for XhoI at the 5′ end and XbaI at the 3′ end. The resulting fragments were cloned in frame into the XhoI and XbaI sites of pEGFP-C3. The fusion proteins contained the GFP at the NH_2 terminus of PTP1B. After verifying all the constructs by sequencing, stable L cell lines were selected with G418. L cells transiently expressing the GFP–PTP1B construct were prepared using Lipofectin, and the cells were processed for analysis after 24–48 h.

Reverse Transcription PCR

Expression of transfected chick PTP1B was assessed by reverse transcription PCR (RT-PCR). In brief, total RNA was isolated from cultured cells using a Qiagen kit (Chatsworth, CA) and reverse transcribed with Superscript II and oligo dT primers (GIBCO BRL). The resulting cDNA was used to amplify PTP1B by two rounds of PCR. Primers used for the first round were specific to the c-myc tag and the chicken PTP1B sequence.

---

1. *Abbreviations used in this paper*: Csk, COOH-terminal Src kinase; FAK, focal adhesion kinase; FN, fibronectin; GFP, green fluorescent protein; LP, parental L cells; LMU, L cells expressing mutant PTP1B; LWT, L cells expressing wild-type PTP1B; PL, polylysine; PTP1B, protein tyrosine phosphatase 1B; PVDF, polyvinylidene fluoride; RT-PCR, reverse transcription PCR.

The first primer set was 5′ GAGCAAAAGCTCATTTCTGAAGAG 3′ from the c-myc tag and 5′ TTCACCAACAGTTCTCCTCC 3′ from the chick PTP1B. The second primer set was 5′ CGCTTAACCCTGAG-TATGGACCTG 3′ (nucleotides 718–727) and 5′ AGCAGTGCTGACT-GAGCATCTTATC 3′ (nucleotides 1154–1130), both from the chick PTP1B sequence (sequence data available from GenBank/EMBL/DDBJ under accession number U86410; Balsamo et al., 1998). For amplification of the mouse β-actin cDNA (accession number X03672), the primers used corresponded to nucleotides 225–278 at the 5′ end and 1023–1003 at the 3′ end.

Flow Cytometry

Surface expression of β1-integrin was analyzed in parental (LP) cells and cells expressing the wild-type (LWT) and mutant (LMU) PTP1B. The cells were grown in culture for 1–2 d and detached by a brief incubation with 0.06% trypsin. The trypsin was inactivated by addition of 1 mM (4-[2-aminoethyl]benzenesulfonylfluoride) (AEBSF; Calbiochem). Cells were collected by centrifugation, resuspended, and incubated in DME/0.1% BSA for 30 min at 4°C. Primary antibodies (20 μg/ml of either rat anti–mouse α5β1-integrin or rat anti–mouse β1-integrin subunit) were then added, and the cells were incubated for an additional 30 min at 4°C. After three washes with DME, the cells were incubated with FITC-conjugated goat anti–rat IgG for 30 min at 4°C, washed three times with DME and once with PBS (137 mM NaCl, 2.7 mM KCl, 10 mM Na$_2$HPO$_4$, 1.8 mM KH$_2$PO$_4$, pH 7.4), and fixed in 3% paraformaldehyde. Fluorescence was analyzed on a Becton Dickinson FACScan® (Bedford, MA). Background fluorescence was assessed in cells immunostained with normal rat IgG (20 μg/ml) as primary antibody, followed by FITC-conjugated goat anti–rat IgG. 5,000 cells per sample were analyzed.

Immunofluorescence Microscopy

LP, LWT, and LMU cells were grown on acid-washed round coverslips (Fisher Scientific) coated with 20 μg/ml fibronectin (FN) (overnight, 4°C). At the indicated times, cells were fixed with 3% paraformaldehyde in PBS for 20 min at 4°C, permeabilized with 0.5% Triton X-100 in PBS for 10 min at room temperature, and blocked with 3% BSA in PBS for 30 min. Cells were then incubated with either of the following monoclonal antibodies: mouse anti-FAK (2.5 μg/ml), mouse antipaxillin (2.5 μg/ml), rat anti-β1-integrin (20 μg/ml), or mouse antivinculin (5 μg/ml). Incubations were carried out in a humid chamber for 1 h at 37°C. Cells were washed three times with PBS and incubated for a similar period with a combination of 0.5 mg/ml TRITC-phalloidin (Sigma Chemical Co.) and 1/60 dilution of either FITC-conjugated donkey anti–mouse IgG or FITC-conjugated goat anti–rat IgG. After washing thoroughly, samples were mounted in 0.1 M Tris-HCl, pH 8.5/glycerol (1:4, vol/vol) containing 1 mg/ml p-phenylendiamine. Stained cells were observed using a universal microscope (Carl Zeiss, Inc., Thornwood, NY) equipped for epifluorescence. Images were captured with a SenSys CCD camera (Photometrics, Tucson, AZ) and analyzed with a Metamorph image analysis system, version 2 (Universal Imaging Corp., West Chester, PA).

Subcellular localization of GFP and GFP–PTP1B fusion proteins was examined with a laser scanning microscope (Carl Zeiss, Inc.) using a 488-nm argon laser. GFP expression was analyzed after paraformaldehyde fixation. For colocalization analysis, cells were fixed and permeabilized as indicated above. In this case, GFP and GFP fusion proteins were detected with a polyclonal anti-GFP antibody followed by an FITC-conjugated donkey anti–rabbit IgG. Images were printed on a color printer (model 8650 PS; Eastman Kodak Corp., Rochester, NY).

Staining of the endoplasmic reticulum was performed using rhodamine B hexyl ester. Living cells were incubated 1 min with 1 μg/ml of the dye, washed three times with PBS, and fixed. Observations were carried out in a confocal microscope using a 543-nm helium-neon laser.

Electrophoresis, Immunoprecipitation, and Western Blots

Cultured cells were rinsed quickly with cold TBS (20 mM Tris-HCl, pH 7.4, 137 mM NaCl) containing 0.5 mM NaVO$_3$ and removed from the culture dish in the same buffer containing 1% Triton X-100, 1 mM PMSF, 10 μg/ml leupeptin, 2.5 mM NaVO$_3$, and 10 mM NaF. Cell lysates were incubated at 4°C for 15 min, with rotation, and then centrifuged for 2 min in a microcentrifuge (Eppendorf, Madison, WI) at maximum speed. Approximately 1 mg of supernatant protein was mixed with 2 μg/ml of either mouse anti-FAK or mouse antipaxillin and incubated with rotation for 3 h at 4°C. Goat anti–mouse IgG conjugated to magnetic beads (PerSeptive Biosystems, Inc., Framingham, MA) was then added, and the suspension was incubated for 1.5 h at 4°C. For β1-integrin immunoprecipitation, ∼2 mg of supernatant protein was first diluted with 1 vol of TBS and incubated with 3 μg/ml of rat anti–mouse β1 antibody followed by goat anti–rat IgG conjugated to magnetic beads. Immunocomplexes were collected and washed three times with TBS/0.5% NP-40 and once with TBS, both containing the protease and phosphatase inhibitors at the concentrations indicated above. Final pellets were resuspended in sample buffer (Laemmli, 1970) and boiled for 5 min, and the beads were pulled down by centrifugation. The resulting supernatant was subjected to SDS-PAGE (8% acrylamide gels) and transferred to polyvinyl difluoride (PVDF) membranes (Bio-Rad Labs, Hercules, CA). After blocking in TBS containing 3% BSA and 0.2% Tween 20 for 90 min at room temperature, membranes were washed briefly with TBS and incubated for 1 h at 37°C with the primary antibody: 1 μg/ml antiphosphotyrosine antibody, 1/600 dilution of anti–β1-integrin antiserum (Giancotti and Ruoslahti, 1990), or 2 μg/ml anti-PTP1B polyclonal IgG. Blots were washed three times with TBS/Tween 20 and once with TBS, and incubated 1 h with the appropriate HRP-conjugated anti-IgG antibody. For determining the levels of phosphotyrosine on Src, cells were serum starved for 2 h, plated on FN-coated dishes, and harvested in RIPA buffer (0.1% SDS, 0.1% deoxycholate, 1% NP-40, 10 mM Tris, pH 7.4, 150 mM NaCl, 2 mM EDTA, 5 mM NaF) with 2.5 mM o-vanadate, 1 mM PMSF, 5 μg/ml leupeptin, and 10 μg/ml DNase. The lysates were centrifuged as above, and the supernatant was incubated with 2 μg/ml rabbit IgG or anti-Src antibody for 4 h at 4°C. The immunocomplexes were collected with goat anti–rabbit magnetic beads and washed and processed as above. Membranes were developed using the ECL system (Amersham Corp., Arlington Heights, IL). To reuse the membranes, they were first incubated in TBS containing 5% 2-mercaptoethanol and 2% SDS for 30 min at 55°C and then thoroughly washed with TBS, blocked again, and probed with a different antibody.

The anti-Src immunoprecipitates were also used to estimate the relative activity of Src from each of the cell lines. The immunoprecipitates were separated by SDS-PAGE and transferred to nitrocellulose. The membrane was incubated for 30 min in two changes of TBS containing 10 mM Mg^{++}, and the Src-containing band (∼0.5 cm) was removed and incubated with 8 μg recombinant mutant GST-chkPTP1B in 250 μl of TBS containing 10 mM Mg^{++}, 0.5 mM DTT, 25 μM ATP, and 0.4 mM o-vanadate for 30 min at 37°C. The reaction was stopped by addition of 50 μl of 5× SDS sample buffer, and the samples were boiled for 2 min. The samples were separated by SDS-PAGE, transferred to PVDF membranes and immunoblotted with anti-PY antibody 4G10. To determine the amount of substrate in each lane, the immunoblot was stripped and reblotted with anti-PTP1B antibody.

Adhesion and Spreading Assays

96-well Falcon polystyrene tissue culture plates (Becton Dickinson) were coated overnight at 4°C with either 20 μg/ml bovine plasma FN (Calbiochem), 250 μg/ml polylysine (PL), or 1% BSA and washed with PBS. FN- and PL-coated wells were blocked for 1 h at 37°C with 1% BSA before use. LP, LWT, and LMU cells grown overnight in serum-free medium were detached with trypsin as indicated above. 20,000 cells were added per well in HBSGK buffer (20 mM Hepes, pH 7.2, 150 mM NaCl, 3 mM KCl, and 2 mM glucose). To ensure rapid and even distribution of the plated cells onto the bottom of the wells, plates were briefly centrifuged (model GH3.8 rotor; Beckman Instruments, Fullerton, CA). Cells were allowed to attach for 45 min at 37°C. Nonadherent cells were removed by washing with HBSGK, and the number of attached cells was quantitated by crystal violet staining (Bonnekoh et al., 1989). In brief, attached cells were fixed for 10 min with 3% paraformaldehyde, washed with PBS, and stained with a crystal violet solution (0.2%, wt/vol in 10% ethanol, vol/vol) for 10 min. Stained cells were rinsed thoroughly with 0.5 M Tris-HCl, pH 7.8, and resuspended in 50 ml of the same buffer containing 0.5% SDS and 50% ethanol. After 30 min, optical density was quantitated at 585 nm using a microplate reader (Bio-Rad Laboratories). When indicated, cells were preincubated for 20 min on ice with the GRGDSP or GRADSP peptides (1 mM) and plated in the presence of the peptides.

For spreading assays, cells were prepared as above, except that they were plated on fibronectin-coated coverslips. After 30 min, cells were fixed with 3% paraformaldehyde, washed with PBS, and incubated with DiI (10 mM) in the dark for 30 min. Excess dye was washed with PBS, and the cells were mounted in 80% glycerol/PBS. The area of fluorescent cells was measured using a Metamorph image analysis system (Universal Imaging Corp.).
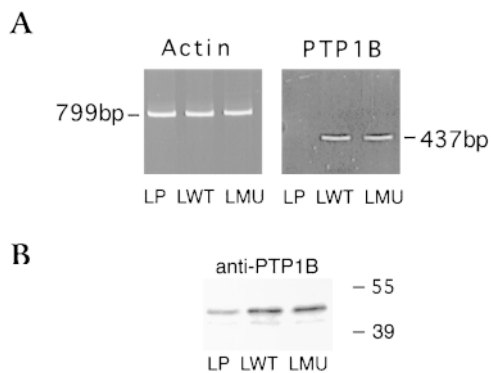
A

B

Figure 1. (*A*) RT-PCR detection of chick PTP1B and β-actin mRNA expression in LP, LWT, or LMU cells. Shown is an ethidium bromide staining. (*B*) PTP1B protein expression. Equal amounts of protein in LP, LWT, or LMU cell homogenates were separated by SDS-PAGE and immunoblotted with anti-PTP1B antibody. Numbers to the right of the figure indicate the migration of prestained molecular mass standards in kilodaltons.

Results

Cell–Substrate Adhesion and Spreading Is Impaired in L Cells Expressing Catalytically Inactive PTP1B

To investigate the role of PTP1B in integrin-mediated adhesion, we transfected L cells with a vector containing the full-length cDNA for chicken PTP1B (wild-type: LWT) or a catalytically inactive form of the phosphatase (C215S: LMU). Both cDNAs carry a c-myc tag in frame at the 5′ end to facilitate subsequent analysis. Stable cell lines were selected with zeocin, and expression of the c-myc–tagged

PTP1B was determined by RT-PCR, using a combination of primers specific to c-myc and the chick enzyme, and by immunoblot. A unique band of 437 bp corresponding to the chick PTP1B message is readily detected in LWT and LMU cells (Fig. 1 *A*). As expected, chick PTP1B message is not detected in LP cells (Fig 1 *A*). Actin message was used to normalize the amount of starting material from each cell preparation (Fig. 1 *A*). PTP1B is readily detected in both control and transfected populations (Fig. 1 *B*). Because we used a pan-specific anti-PTP1B, we were able to estimate the level of overexpression to be about twofold (Fig. 1 *B*).

To assess the effect of transfected wild-type and inactive PTP1B on integrin-mediated adhesion, several clones of LWT and LMU cells as well as LP cells were plated on fibronectin-coated, 96-well plates in serum-free medium, and the attached cells were quantified after 45 min incubation. Only 30% of the input LMU cells adhered, as compared with more than 90% of the LP and LWT cells (Fig. 2 *A*). Attachment of control LP and LWT cells to fibronectin is integrin-dependent: over 90% attachment is inhibited by an RGD-containing peptide (Fig. 2 *A*). Several clones expressing wild type and mutant were analyzed by phase contrast microscopy after culture in the presence of serum. All clones expressing the mutant PTP1B (LMU) are similar and morphologically different from clones expressing the wild-type protein (LWT) or the parental cell line (LP) (Fig. 2 *B*). LMU cells show a bipolar, spindle shape and do not flatten onto the substrate. In contrast, LP and LWT cells form extensive lamellae and are flattened on the matrix (Fig. 2 *B*).

The poor attachment of LMU cells to fibronectin is also reflected in their inability to flatten and spread. 30 min after plating on fibronectin, most LMU cells remain round
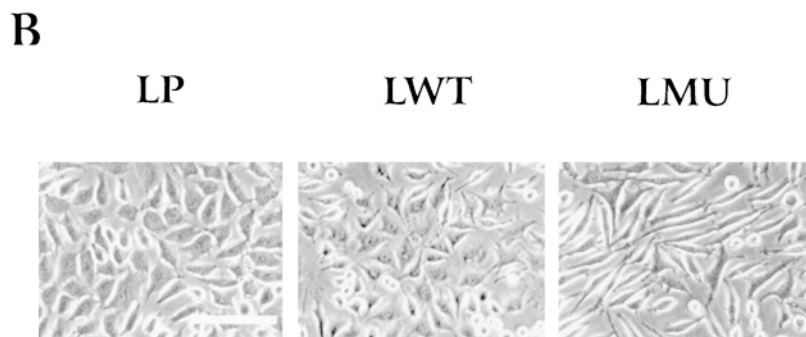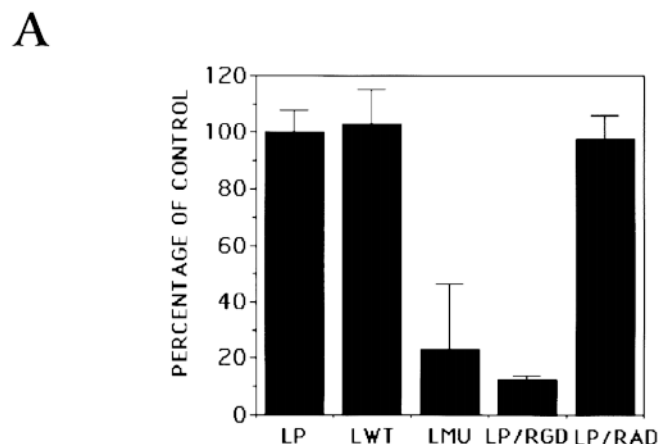
A

B

Figure 2. (*A*) Cell attachment of LP, LWT, and LMU cells to fibronectin. The number of cells attached after 45 min of plating was determined. Values for each condition represent the percentage of attached cells as compared with LP. Error bars are the standard deviation of three independent experiments, each counted in triplicate. Background attachment to BSA-coated wells was subtracted from the experimental values. In LP/RGD and LP/RAD, cells were preincubated 20 min on ice with the GRGDSP or GRADSP peptide (1 mM) and plated in the presence of the peptides. (*B*) Phase contrast images of LP, LWT, and LMU cells cultured in the presence of serum. Note the elongated and thin morphology of LMU cells compared with LWT and LP cells. Bar, 200 μm.
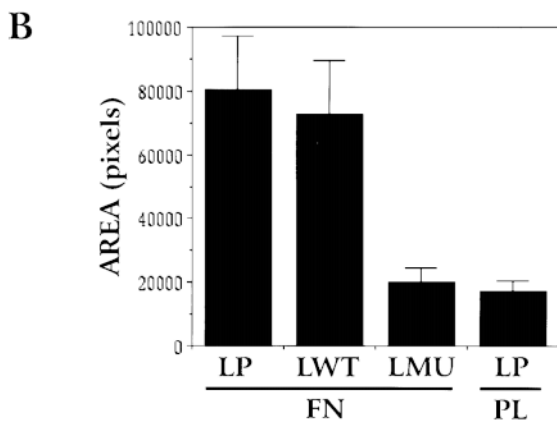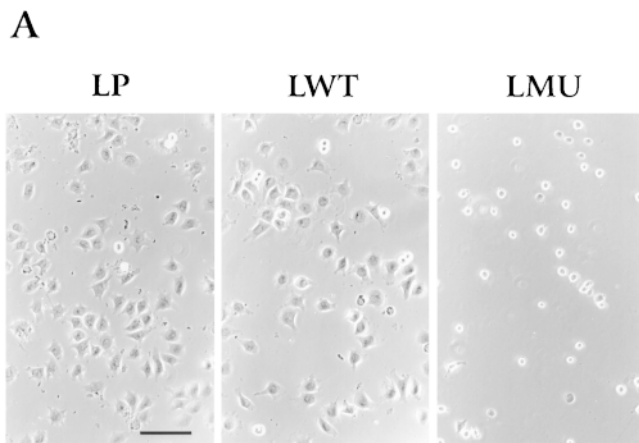
A

LP   LWT   LMU

B

Figure 3. Spreading of LP, LWT, and LMU cells on fibronectin-coated coverslips. Cell spreading was determined after 30 min of plating. (*A*) Phase contrast images. (*B*) Cell area quantitated in pixels using the Metamorph image analysis system. Bar, 160 μm.

α5β1   β1

Figure 4. Flow cytometry analysis of the surface expression of α5β1-integrin fibronectin receptor and β1-integrin subunit in LP, LWT, and LMU cells. Cells were stained with either anti-α5β1 mAb, anti-β1 mAb (dark), or an isotype-matched control immunoglobulin (clear), followed by FITC-conjugated secondary antibody (see Materials and Methods).

and very loosely attached to the substrate, with only a few cells showing limited spreading. In contrast, most of the LP and LWT cells flatten and form large lamella (Fig. 3 *A*). The surface areas of LP and LWT cells are similar and approximately three times that of LMU cells, as determined by quantitative image analysis (Fig. 3 *B*). The reduced attachment and spreading of LMU cells on fibronectin is not due to a decreased expression of integrins at the cell surface since flow cytometry profiles of surface-labeled β1-integrin and the major fibronectin receptor, α5β1, are equivalent in all three cell types (Fig. 4). In addition, immunoblots of cell lysates with anti–mouse β1-integrin antibody show equal levels of expression (not shown).

Focal Adhesions and Actin Stress Fibers Are Altered in L Cells Expressing Catalytically Inactive PTP1B

In normal fibroblasts, integrin-mediated adhesion to fibronectin leads to the formation of focal adhesions and assembly of actin stress fibers (Burridge et al., 1988). The impaired attachment and spreading of LMU cells on fibronectin suggests that these cells may be unable to assemble normal focal contacts and actin stress fibers. To investigate this possibility, LMU cells were plated on fibronectin for 30 min and then fixed and processed for
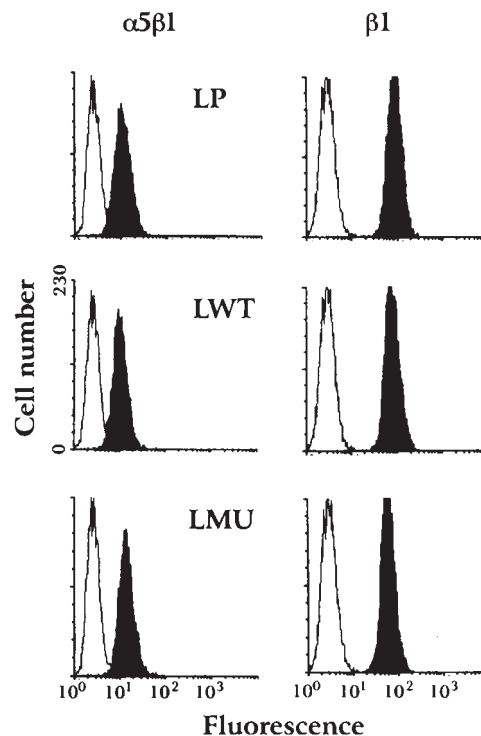
double immunofluorescence to detect F-actin and β1-integrin. Actin appears diffusely distributed throughout the cell body but accumulates in the submembranal cytoskeleton (Fig. 5 *A*). β1-integrin is distributed uniformly in a diffuse pattern all over the cell, with occasional small aggregates (Fig. 5 *B*). In contrast, among LWT cells, actin is organized in stress fibers (Fig. 5 *C*), and β1-integrin accumulates in focal contacts (Fig. 5 *D*).

To determine if LMU cells have a delayed ability to assemble stress fibers and focal contacts, cells were plated on fibronectin and cultured for 2 d in the presence of serum before staining with TRITC-phalloidin and anti-β1 antibody. After this time, most LMU cells have an elongated shape but still lack actin stress fibers and focal adhesions. Actin is distributed in short filaments within the cell body and in the submembranal cytoskeleton (Fig. 6 *A*). Actin filaments are also seen aligned along the main axis of the cells and following a radial pattern within the lamellipodia (Fig. 6, *A* and *C*). β1-integrin is distributed in a dotted pattern, with only a few small accumulations at or near the cell margin and very weak staining in some lamellipodia (Fig. 6, *B* and *D*). As expected, in LWT and LP cells actin accumulates in prominent stress fibers and β1-integrin in focal adhesions (Fig. 6, LWT: *E* and *F*; LP: *G* and *H*).

The distributions of other typical focal adhesion components, such as FAK, paxillin, and vinculin, are also altered in LMU cells. In all cases, the distribution is dotted, with occasional formation of small aggregates (Fig. 7). In con-
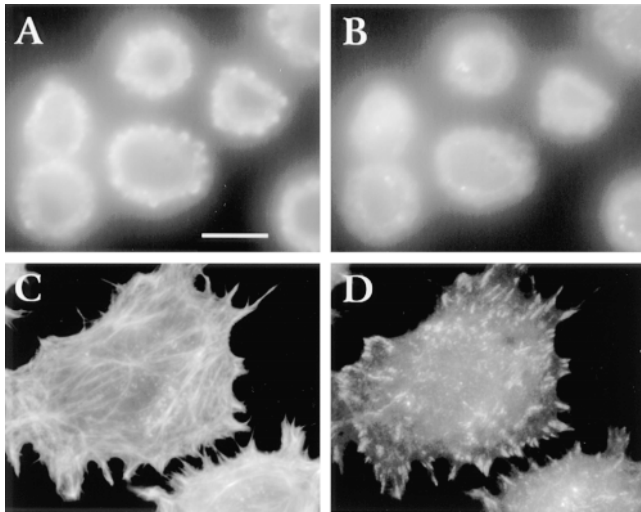
Figure 5. Distribution of β1-integrin and actin in cells plated for 30 min on fibronectin. Serum-starved LMU (*A* and *B*) and LWT (*C* and *D*) cells in DME were plated on fibronectin-coated coverslips and fixed 30 min later. The cells were processed for double immunofluorescence staining with rat anti–mouse β1 mAb/FITC-goat anti–rat IgG (*B* and *D*) and TRITC-phalloidin (*A* and *C*). Note the lack of spreading, focal contacts, and actin stress fibers in LMU cells. Bar, 15 μm.

trast, these proteins are distributed in large and elongated focal adhesions in LWT (Fig. 7) and LP cells (not shown).

Tyrosine Phosphorylation of FAK and Paxillin Is Reduced in L Cells Expressing Catalytically Inactive PTP1B

Tyrosine phosphorylation of FAK is an early event occurring after integrin binding to the ligand (Guan and Shalloway, 1992; Lipfert et al., 1992; Kornberg et al., 1992; Clark and Brugge, 1995). To examine whether phosphorylation of FAK on tyrosine residues is affected in LMU cells, nonionic detergent extracts of cells plated on polylysine or fibronectin for 30 min were immunoprecipitated with an anti-FAK antibody and immunoblotted with an antiphosphotyrosine antibody. On polylysine, phosphotyrosine levels on FAK are barely detectable in the three cell lines (not shown). On fibronectin, phosphotyrosine levels in FAK are significantly reduced in LMU cells as compared with those in LP and LWT cells (Fig. 8 *A*, *top*), suggesting that phosphorylation of FAK on tyrosine residues in response to the attachment to fibronectin is indeed impaired in LMU cells.

Similarly, paxillin is localized in focal adhesions and becomes tyrosine phosphorylated after integrin-dependent adhesion (Burridge et al., 1992). To determine whether phosphorylation of paxillin on tyrosine is also affected in LMU cells, lysates from cells plated on fibronectin were immunoprecipitated with a specific antipaxillin antibody, and phosphotyrosine residues were detected as described above. Indeed, in LMU cells, paxillin shows reduced levels of phosphotyrosine when compared with LP and LWT cells (Fig. 8 *B*, *top*). The reduced phosphorylation of FAK and paxillin in LMU cells cannot be attributed to a lower level of protein expression or to differential immunopre-
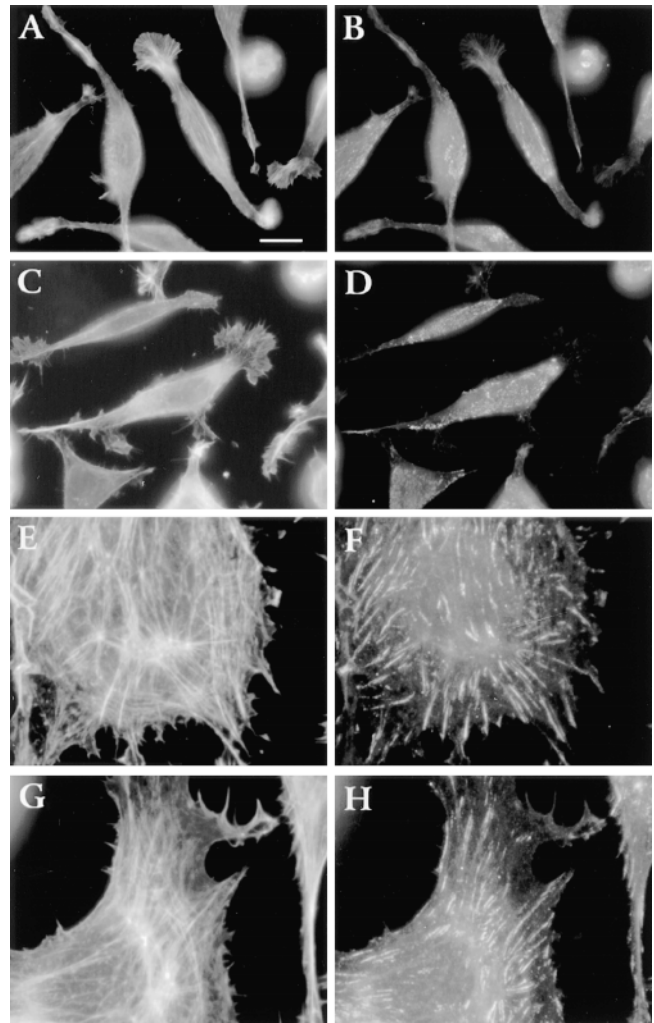

Figure 6. Distribution of β1-integrin and actin in cells cultured for 2 d. LMU (*A–D*), LWT (*E* and *F*), and LP (*G* and *H*) cells in DME/FBS were plated on fibronectin-coated coverslips. After 2 d, cells were fixed, permeabilized, and double stained with rat anti–β1 mAb/FITC-goat anti–rat IgG (*B*, *D*, *F*, and *H*) and TRITC-phalloidin (*A*, *C*, *E*, and *G*). Bar, 10 μm.

cipitation since equivalent amounts of protein were used for all immunoprecipitations, and the amount of immunoprecipitated FAK and paxillin is similar in the three cell lines, as determined by stripping the membranes and blotting with anti-FAK (Fig. 8 *A*, *bottom*) or antipaxillin (Fig. 8 *B*, *bottom*) antibodies.

To eliminate the possibility that a general dephosphorylation of proteins occurs in cells expressing the mutant PTP1B, lysates from cells plated on fibronectin were fractionated by SDS-PAGE, transferred to PVDF membrane, and immunoblotted with antiphosphotyrosine antibody. Tyrosine phosphate residues at the appropriate molecular mass for FAK and paxillin are reduced in LMU cells (Fig. 8 *C*). There are changes in the phosphorylation levels of other proteins in LMU cells; however, there are no wholesale changes in the pattern. It is of interest that phosphorylation of high (∼200 kD) and low (∼30 kD) molecular mass bands are reduced in LWT cells, indicating that in-
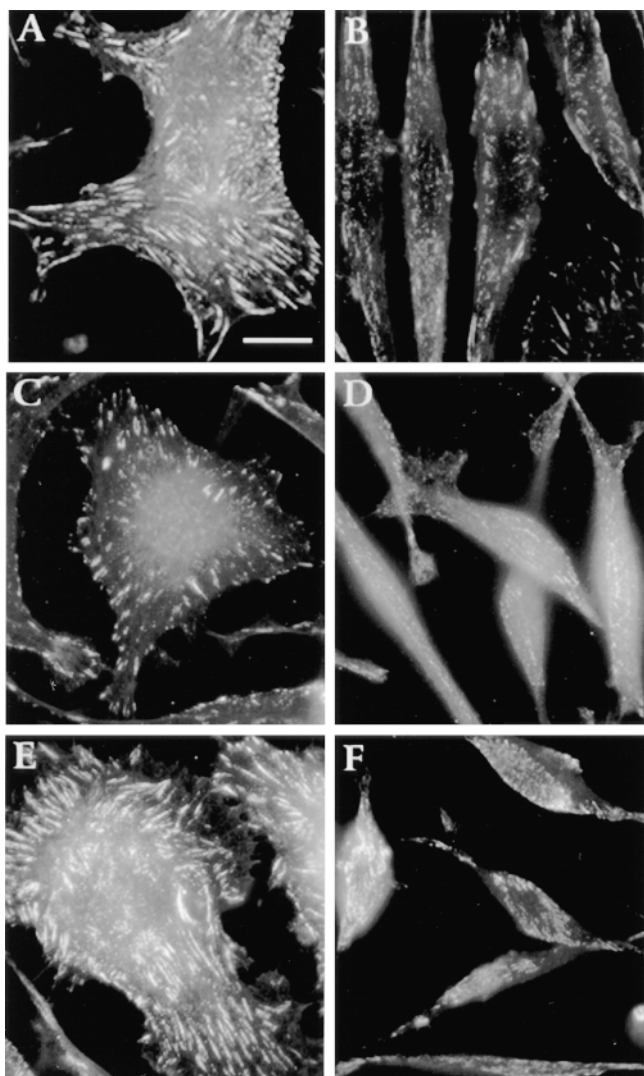
Figure 7. Distribution of FAK, paxillin, and vinculin in LMU and LWT cells plated on fibronectin-coated coverslips. LWT (*A*, *C*, and *E*) and LMU (*B*, *D*, and *F*) cells cultured for 2 d were fixed and processed for immunofluorescence using monoclonal antibodies against paxillin (*A* and *B*), FAK (*C* and *D*), or vinculin (*E* and *F*). Bar, 20 μm.

Figure 8. Phosphotyrosine levels of FAK and paxillin in LP, LWT, and LMU cells. LP, LWT, and LMU cells were plated on fibronectin for 30 min, lysed (see Materials and Methods), and immunoprecipitated (*IP*) with (*A*) anti-FAK mAb or (*B*) anti-paxillin mAb and immunoblotted (*IB*) with antiphosphotyrosine (*PY*) antibody. Lower panels show stripped membranes reblotted with the same antibodies used for immunoprecipitation. (*C*) Phosphotyrosine staining of total proteins in Triton X-100 lysates. LP, LWT, and LMU cells plated on fibronectin for 30 min were lysed as described in Materials and Methods. Numbers at the left indicate the position of molecular mass markers in kilodaltons.

creased levels of active PTP1B does alter the pattern of phosphorylation.

Tyrosine Phosphorylation of Src Is Increased and Activity Decreased in L Cells Expressing Catalytically Inactive PTP1B

The decrease in tyrosine phosphorylation of FAK and paxillin in cells expressing the catalytically inactive PTP1B indicates that PTP1B plays a role in regulating the tyrosine phosphorylation of components upstream from these phosphorylation events. Src is an obvious candidate since FAK and paxillin are downstream targets of Src (Clark and Brugge, 1993; Howel and Cooper, 1994; Kaplan et al., 1994; Calalb et al., 1995; Schaller and Parsons, 1995; Hanks and Polte, 1997). Tyrosine 527 must be dephosphorylated to activate Src (Courtneidge, 1985; Cooper and
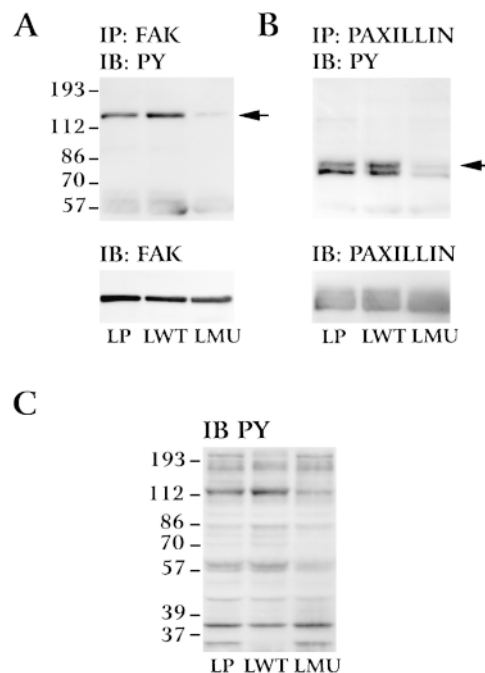
King, 1986; Brown and Cooper, 1996) and mutant PTP1B may block this event. An increase in tyrosine phosphate content of Src has been correlated with decreased activity (Soltesz et al., 1997). To assess the tyrosine phosphate content of Src, extracts of cells plated on fibronectin for 1 h were immunoprecipitated with an anti-Src antibody and immunoblotted with an antiphosphotyrosine antibody. The phosphotyrosine content of Src is increased in the LMU cells as compared with LP cells (Fig. 9 *A*). It is interesting to note that overexpression of wild-type PTP1B decreases the phosphotyrosine content of Src, without an apparent alteration of the phenotype (Fig. 9 *A*). The amount of Src in each lane is also shown (Fig. 9 *A*, *bottom*).

To directly estimate the relative activity of Src in each of the cell types, Src was immunoprecipitated and assayed in vitro using mutant chk-PTP1B as the substrate (Jung et al., 1998). Transfer of phosphate to the substrate was determined by SDS-PAGE and immunoblot with anti-PY antibody (Fig. 9 *B*). Src isolated from LMU cells is clearly less active than that isolated from either LP or LWT cells.

Subcellular Distribution of PTP1B

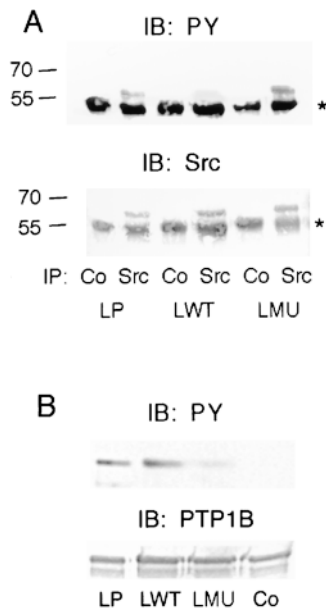It has been shown that PTP1B is predominantly localized in the endoplasmic reticulum (ER) (Frangioni et al., 1992;

Figure 9. Comparison of phosphotyrosine levels and activity of Src in LP, LWT, and LMU cells. (*A*) Phosphotyrosine levels: serum-starved LP, LWT, and LMU cells were plated on fibronectin-coated plates and incubated for 1 h at 37°C. The cells were homogenized in RIPA buffer, immunoprecipitated with anti-Src antibody or control rabbit IgG (*Co*), and immunoblotted with antiphosphotyrosine mAb 4G10. The membrane was stripped and reblotted with anti-Src antibody. An asterisk to the right indicates the migration of IgG heavy chain. Numbers to the left indicate the position of molecular mass markers in kilodaltons. (*B*) Src activity: the anti-Src immunoprecipitates were assayed for kinase activity using recombinant, mutant, GST-chkPTP1B as substrate. The reaction mix was separated by SDS-PAGE, transferred to PVDF membranes, and immunoblotted with mAb 4G10. The same membranes were stripped and reblotted with anti-PTP1B antibody. *Co*, LP cells immunoprecipitated with control rabbit IgG.

Woodford-Thomas et al., 1992). To investigate whether a fraction of PTP1B is associated with integrin complexes, nonionic detergent extracts of LWT and LMU cells plated for 30 min on fibronectin were immunoprecipitated with a rat anti–β1-integrin antibody, and the precipitates were analyzed for the presence of PTP1B after SDS-PAGE and immunoblot. Rabbit anti-PTP1B antibody reveals a band at 50 kD, the approximate molecular mass for the intact chicken PTP1B protein (Fig. 10 *A*). This band is not present in control immunoprecipitates. To confirm the
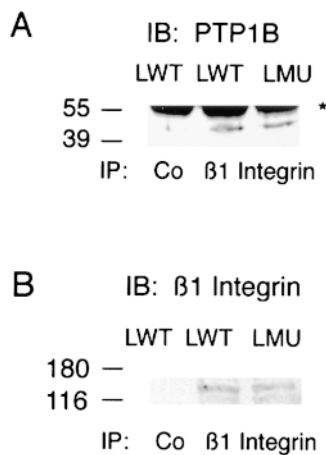

Figure 10. PTP1B coimmunoprecipitation with β1-integrin. (*A*) LWT and LMU cells were lysed in nonionic detergent and immunoprecipitated with a rat anti–β1 antibody or normal rat IgG (*Co*). After separation by SDS-PAGE and transfer to PVDF membranes, the immunoprecipitates were reacted with a rabbit anti–PTP1B and developed with HRP-conjugated anti–rabbit antibody. (*B*) The membranes were stripped and reblotted with anti–β1-integrin antibody. An asterisk to the right indicates the migration of IgG heavy chain. Numbers at the left indicate the position of molecular mass markers in kilodaltons.
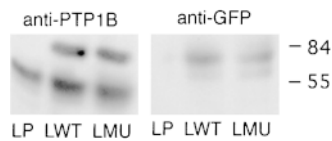

Figure 11. Expression of GFP–PTP1B. L cells were transfected with GFP–wtPTP1B, GFP–mutPTP1B, or GFP alone. The cells were homogenized in RIPA buffer, separated by SDS-PAGE, and immunoblotted with anti-PTP1B antibody or anti-GFP antibody. Numbers at the right indicate the position of molecular mass markers in kilodaltons.

immunoprecipitation of β1-integrin, blots were probed with a polyclonal anti-β1 antibody (Fig. 10 *B*).

In an alternative approach, L cells were transiently transfected with wild-type and catalytically inactive (C215S) forms of chick PTP1B tagged with the green fluorescent protein at the NH$_2$ terminus. The cells were analyzed for expression of the GFP–PTP1B construct by immunoblot with anti-PTP1B antibody and anti-GFP antibody (Fig. 11). Parental PTP1B migrates at ~50 kD, while the GFP fusion migrates at ~77 kD (27 kD + 50 kD). The anti-GFP antibody recognizes the band at ~77 kD as expected. Among cells that express high levels of GFP–wtPTP1B and GFP–mutPTP1B, both proteins are seen in a pattern typical for the ER as revealed by staining with the ER marker rhodamine B hexyl ester (Terasaki and Reese, 1992) (Fig. 12, compare *A* and *B* with *D*). In contrast, cells transfected with the GFP alone show a uniform distribution of the GFP (Fig. 12 *C*). These results indicate that the GFP tag does not significantly affect the targeting of PTP1B to the ER, a subcellular localization previously reported for endogenous PTP1B (Frangioni et al., 1992; Woodford-Thomas et al., 1992).
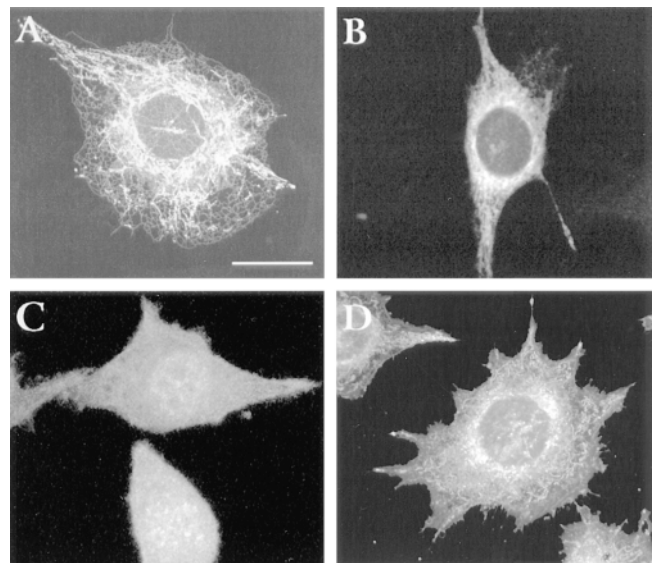

Figure 12. Immunolocalization of GFP–wtPTP1B (*A*), GFP–mutPTP1B (*B*), and GFP alone (*C*) in L cells. L cells were transiently transfected and fixed 48 h later. For comparison, untransfected cells were stained with rhodamine B hexyl ester, a marker of the endoplasmic reticulum (*D*). Note that both wtPTP1B and mutPTP1B target predominantly to the ER. A single 1-μm optical section is shown for all fields. Bar, 30 μm.
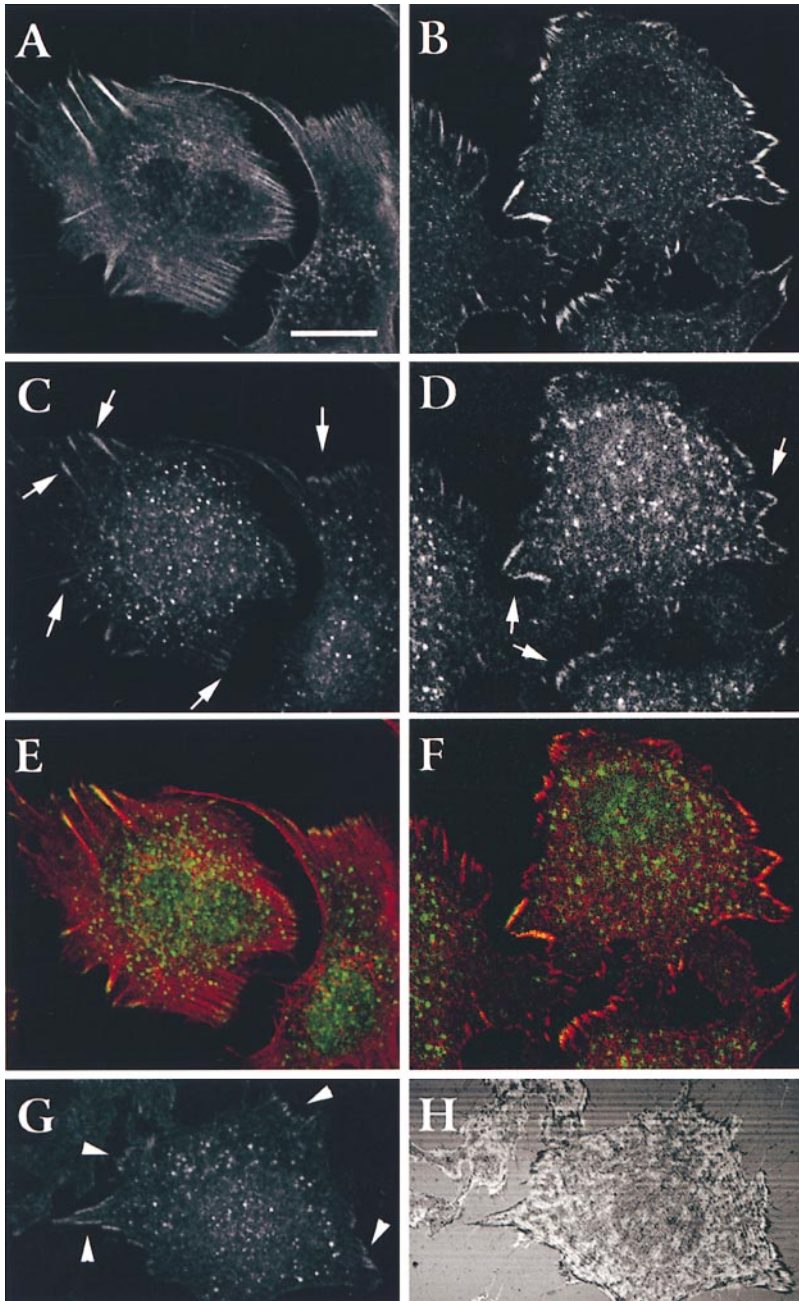
Figure 13. Localization of wtPTP1B in focal adhesions. L cells were transiently transfected with GFP–wtPTP1B and fixed 48 h later. Cells stained with TRITC-phalloidin (*A*) or with a monoclonal antivinculin antibody followed by a rhodamine-anti–mouse antibody (*B*) were double stained with an anti-GFP polyclonal antibody followed by a FITC-anti–rabbit antibody (*C* and *D*). The distribution of the fluorescence in 1-μm-thick optical sections was examined by confocal microscopy. Arrows (*C* and *D*) show sites of overlapping staining at the tips of actin stress fibers and focal adhesions. Color images (*E* and *F*) show overlapping of the staining between actin-PTP1B (*E*) and vinculin-PTP1B (*F*). Orange and yellow indicates regions of overlapping. Anti-GFP staining (*G*) was compared with the pattern obtained by interference reflection microscopy (*H*). Arrowheads indicate the codistribution of the GFP–wtPTP1B with dark regions at the margins of the cell and where cell membrane form extensive focal adhesions. Bar, 25 μm.

Among cells that express moderate or low levels of GFP–wtPTP1B, localization at focal adhesions is observed. To confirm this, double immunofluorescence analyses were performed comparing the distribution of the GFP–wtPTP1B with that of vinculin and actin, two prominent components of focal adhesions. Analysis of 1-μm optical sections taken at the cell–substrate level shows that GFP–wtPTP1B colocalizes with actin at the ends of the stress fibers (Fig. 13, *arrows* in *C*, and compare with *A*). GFP–wtPTP1B also shows a high degree of colocalization with vinculin (Fig. 13, *arrows* in *D*, and compare with *B*).

In addition, GFP–wtPTP1B staining was compared with images taken by reflection interference microscopy, where the pattern of focal adhesions is revealed. The overlap between the immunofluorescence of GFP–wtPTP1B and the dark regions at the margins of cellular lamella seen by reflection interference optics indicates that wtPTP1B localizes in areas of focal adhesions (Fig. 13, *arrowheads*). Similar results are seen using anti-PTP1B antibody (not shown).

Lysophosphatidic Acid Stimulates Assembly of Focal Adhesions in LMU Cells

Growth factors present in serum, such as lysophosphatidic acid, induce the assembly of focal contacts and actin stress fibers, as well as increase the phosphorylation of FAK and paxillin on tyrosine residues (Ridley and Hall, 1992; Zachary et al., 1993; Seufferlein and Rozengurt, 1994). To determine whether expression of the mutant PTP1B also af-
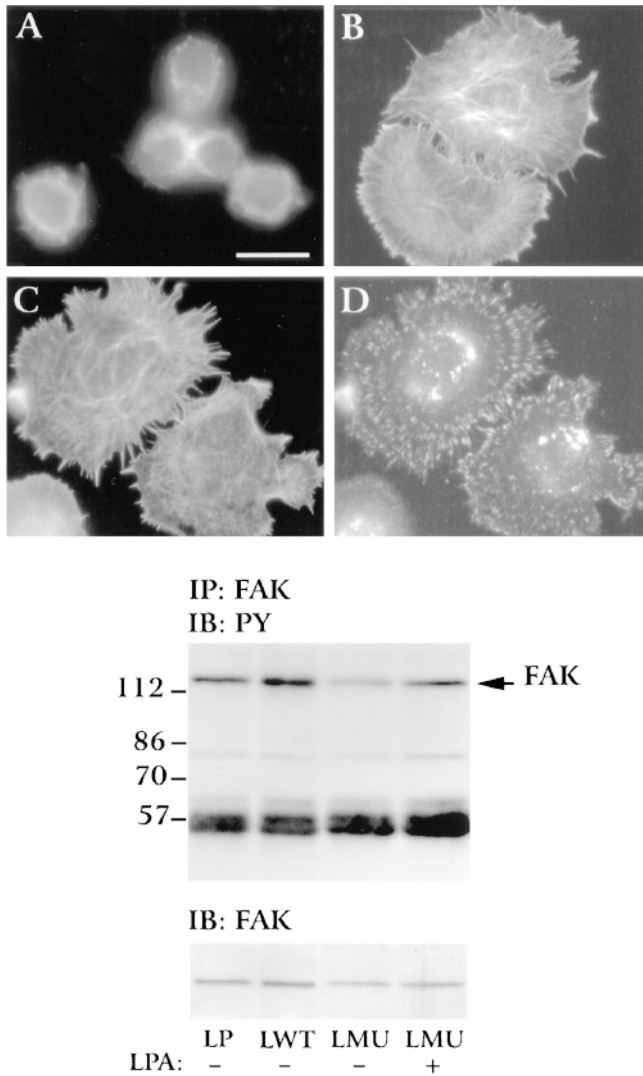
IP: FAK
IB: PY

112 — ← FAK

86 —
70 —
57 —

IB: FAK

LP LWT LMU LMU
LPA: −   −   −   +

Figure 14. Effect of lysophosphatidic acid in LMU cells. Serum-starved cells were plated in DME on fibronectin-coated coverslips in the absence or presence of 200 ng/ml lysophosphatidic acid and fixed after 15 min. Cells were permeabilized and stained with rat anti–β1 antibody (*D*) and TRITC-phalloidin labeled (*A–C*). Anti–β1-integrin staining was visualized by a FITC-conjugated goat anti–rat IgG. (*A*) LMU cells plated in the absence of LPA. (*B*) LWT cells plated in the absence of LPA. (*C* and *D*) LMU cells exposed to LPA and stained for actin (*C*) or β1-integrin (*D*). Note the formation of actin stress fiber (*C*) and induction of focal contacts (*D*) in LMU cells exposed to LPA. Tyrosine phosphorylation of FAK is shown in the immunoblot below. LP, LWT, and LMU cells were plated on fibronectin, lysed after 15 min under denaturing conditions, and immunoprecipitated with anti-FAK antibody. The immunoprecipitates were fractionated by SDS-PAGE and analyzed by immunoblotting with the 4G10 monoclonal antiphosphotyrosine antibody. Note the difference in the phosphorylation of FAK when LMU cells were plated in the absence or presence of LPA. The bottom panel shows the same blot stripped and probed with anti-FAK antibody. Numbers at the left indicate the position of molecular mass markers in kilodaltons. Bar, 20 μm.

fects the LPA-dependent signaling pathway, LMU cells were plated on fibronectin in the presence or absence of LPA. In the presence of LPA, LMU cells rapidly flatten and produce extensive lamella (Fig. 14, compare *A* with *C*). The area of spreading among LMU cells in the presence of LPA is equivalent to that of LWT cells (Fig. 14, compare *B* with *C*) or LP cells (not shown) as determined by quantitative image analysis. Moreover, in LMU cells treated with LPA, β1-integrin and F-actin show their typical distribution in focal contacts and stress fibers (Fig. 14, *C* and *D*). The distribution of vinculin and FAK is similar to that of β1-integrin (not shown).

To determine whether there is an increase in phosphorylation of FAK on tyrosine residues as a response to LPA, nonionic detergent lysates of LMU cells were immunoprecipitated with anti-FAK antibody, and the precipitates were separated by SDS-PAGE and immunoblotted with antiphosphotyrosine antibody. 15 min after plating LMU cells on fibronectin, in the presence of LPA, the levels of phosphorylated tyrosine residues on FAK are similar to those in LP cells (Fig. 14). The effects of LPA in inducing spreading, focal contact and stress fiber formation, and FAK phosphorylation require integrin ligation since they are not observed in cells grown on polylysine (not shown). The rapid response of LMU cells to LPA treatment rules out the possibility that the machinery essential for phosphorylation of FAK and paxillin and for assembly of focal contacts and stress fibers is defective in LMU cells.

Discussion

In this paper, we present data that suggest a regulatory role for PTP1B in integrin-mediated adhesion and spreading. L cells expressing a catalytically inactive form of PTP1B display reduced attachment and are unable to spread on fibronectin. They assume an elongated spindle shape after prolonged culture but fail to form the typical flattened phenotype. Consistent with this altered morphology, LMU cells also show a dramatic decrease in focal adhesions and actin stress fibers. They are able, however, to assemble actin into long filaments parallel to the long axis of the cell and short filaments in the submembrane region of cells and lamellipodia. Additionally, the proportion of polymeric actin in LMU cells is similar to that in LWT or LP cells (Arregui, C.O., unpublished observation). The level of expression of β1-integrin at the cell surface is unaltered in LMU cells; however, its distribution changes to a dotted pattern that contrasts with that of morphologically differentiated focal adhesion complexes in control cells.

Since activated rho is required for the assembly of focal adhesions and actin stress fibers (Ridley and Hall, 1992; Barry and Critchley, 1994; Nobes and Hall, 1995), we considered the possibility that rho-dependent signaling could be impaired in LMU cells. However, when incubated with serum or lysophosphatidic acid, both of which activate the rho pathway (Ridley and Hall, 1992), LMU cells rapidly acquire a phenotype similar to parental or LWT cells, indicating that the machinery to assemble actin stress fibers and focal adhesions is intact. The effect of LPA or serum is dramatic but transient, since cells cultured for longer periods do not retain the spread shape and do not develop focal adhesions and stress fibers. Thus, the normal interac-

tion of integrins with the extracellular matrix appears to be essential for the sustained development of focal adhesions and stress fiber assembly. Our results are in concert with a recent report showing that neither rho nor the extracellular matrix alone are sufficient to sustain focal adhesions in 3T3 cells (Hotchin and Hall, 1995).

PTP1B as Modulator of Integrin-mediated Adhesion

Focal adhesion complexes contain many components, some of which serve structural roles, forming the actual adhesion and links to the actin-based cytoskeleton. Other components of the complex serve to propagate signals initiated outside the cell by ligation of integrins, or those initiated by growth factors and activation of integrins from inside the cell (for reviews see Burridge and Chrzanowska-Wodnicka, 1996; Machesky and Hall, 1996). Furthermore, it is clear that there is redundancy of function among components of focal adhesion complexes (Soriano et al., 1991; Ilic et al., 1995; Thomas et al., 1995). It is important to emphasize that, given this complexity, interruption of the signaling pathway(s) leading to loss of focal contact formation may result in several different phenotypes with respect to the phosphorylation of focal contact components, or even the array of components associated with integrin adhesion complexes. These phenotypes will depend on the point at which the signal cascade is interrupted.

Src is an obvious target for the effect of the dominant-negative PTP1B. FAK and paxillin are downstream targets of Src (Clark and Brugge, 1993; Howel and Cooper, 1994; Kaplan et al., 1994; Calalb et al., 1995; Schaller and Parsons, 1995; Hanks and Polte, 1997), and the enzymatic activity of Src is regulated by the balance of phosphorylation/dephosphorylation of tyrosine 527. The COOH-terminal Src kinase (Csk) phosphorylates tyrosine 527 and represses Src activity (Nada et al., 1991, 1993; Okada et al., 1991; Imamoto and Soriano, 1993), and activation requires dephosphorylation of this residue (Courtneidge, 1985; Cooper and King, 1986; Brown and Cooper, 1996). This may be accomplished by the cytosolic tyrosine phosphatase SHP-1 (Somani et al., 1997) and possibly the transmembrane tyrosine phosphatase PTPα (Fang et al., 1994). We are suggesting that PTP1B may also play such a role. Our results are consistent with this hypothesis; transfection with the dominant-negative, catalytically inactive PTP1B results in increased phosphotyrosine content of Src and decreased activity, presumably by preventing the dephosphorylation of Tyr 527 by endogenous PTP1B or other phosphatases, keeping Src in a repressed state (see Fig. 15).

Several additional lines of evidence are also consistent with the hypothesis that the reduced levels of tyrosine phosphorylation of FAK and paxillin in LMU cells are due to repression of Src. Recruitment of Src to focal adhesions follows integrin engagement (Clark and Brugge, 1993; Kaplan et al., 1995) and is accompanied by a transient increase in Src activity concomitant with a decrease in the phosphorylation of Tyr 527 (Clark and Brugge, 1993; Kaplan et al., 1995). FAK and paxillin tyrosine phosphorylation is increased in cells isolated from Csk-minus mice (Thomas et al., 1995), and overexpression of Csk in HeLa cells results in impaired cell–substrate adhesion and
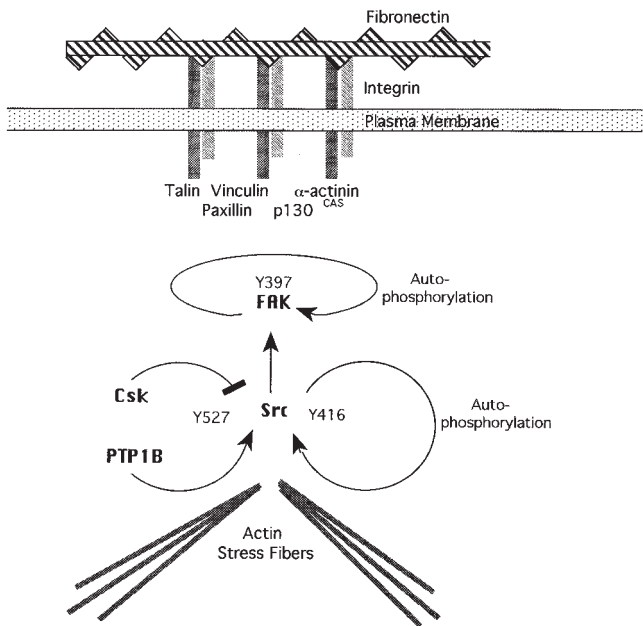

Figure 15. Scheme showing a possible mechanism of action for PTP1B. Arrows indicate stimulatory interactions, and blunt lines indicate inhibitory interactions. The COOH-terminal Src tyrosine kinase, Csk, phosphorylates Y527-repressing Src activity. Activation of Src occurs by autophosphorylation of Y416 and dephosphorylation of Y527. Dephosphorylation of Y527 by PTP1B would therefore contribute to Src activation. Src, in turn, phosphorylates FAK and other components of the focal adhesion complex. The dominant-negative PTP1B would decrease dephosphorylation of Y527, maintaining Src in a repressed state.

spreading and a redistribution of integrins from focal contacts to point contacts (Bergman et al., 1995), a phenotype similar to our L cells expressing mutant PTP1B. Finally, fibroblasts from Src knock out mice also show reduced spreading (Kaplan et al., 1995).

In seeming contrast to our results, Liu et al. (1998) have reported that introduction of wild-type PTP1B into 3Y1 fibroblasts reduces the rate of cell spreading and ultimately results in the formation of abnormally dense bundles of stress fibers and enlarged, elongated focal contacts. This was accompanied by reduced levels of phosphorylation of FAK (Liu et al., 1998). We do not see an effect of wild-type PTP1B on adhesion or focal contacts in L cells. In agreement with our observations, spreading and cytoskeletal organization are not altered by expression of wild-type PTP1B in human foreskin fibroblasts or W-87MG glioblastoma cells (Tamura et al., 1998). Interestingly, we do see a significant enhancement of neurite outgrowth by PC12 cells expressing wild-type PTP1B (Pathre, P., C. Arregui, J. Lilien, and J. Balsamo, manuscript in preparation). This may reflect effects similar to those seen by Liu et al. (1998), a possibility we are investigating. The different phenotypes resulting from perturbation of PTP1B may therefore be due to differences in host cell type and/or expression levels or PTP1B.

Subcellular Distribution of PTP1B

We find that PTP1B coimmunoprecipitates with β1-inte-

grin, colocalizes with vinculin and actin—two prominent components of focal adhesions—and is present in focal adhesions. These data suggest that PTP1B interacts with one or more components of focal adhesion complexes. One candidate molecule is p130Cas. Human PTP1B has been shown to bind to p130 Cas both in vitro and in intact cells. Binding occurs through a proline-rich region near the COOH terminus of PTP1B and the SH3 domain of p130Cas (Liu et al., 1996, 1998). It is interesting that other tyrosine phosphatases also interact with p130Cas (Black and Bliska, 1997; Garton et al., 1997; Shen et al., 1998).

Like targeting to p130Cas, the proline-rich region of PTP1B may also interact with the SH3 domain of Src itself. The selective dephosphorylation of Tyr 527 over 416 may be due to sequence recognition by PTP1B—tyrosines 527 and 416 of Src are presented in entirely different sequence motifs (Takeya and Hanafusa, 1983)—and/or accessibility based on targeting. It is worth emphasizing that targeting mechanisms can impose limits on the available protein substrates and specific tyrosine residues.

The Many Faces of PTP1B

Full-length PTP1B was initially described as localized to the endoplasmic reticulum (Frangioni et al., 1992; Woodford-Thomas et al., 1992). PTP1B has also been reported to interact with both the insulin and IGF-1 receptors regulating the ligand-induced signaling via these receptors (Kenner et al., 1996; Seely et al., 1996; Bandyopadhyay et al., 1997). It also interacts with and is phosphorylated by the EGF receptor (Milarski, et al., 1993; Flint et al., 1997; Liu and Chernoff, 1997). Here we report that PTP1B is functionally and physically associated with focal contacts. We have also reported that, in chick neural retina cells and in L cells stably expressing N-cadherin, a fraction of PTP1B binds to N-cadherin and regulates its function through dephosphorylation of β-catenin (Balsamo et al., 1996; Balsamo et al., 1998). PTP1B thus plays multiple roles depending on specific interactions, whether via substrate recognition or other specific targeting regions of the molecule.

Finally, it is interesting to note that PTP1B plays an important role in regulating both integrin adhesion complexes (Liu et al., 1998; this paper) and cadherin adhesion complexes (Balsamo et al., 1996; Balsamo et al., 1998). This suggests possibilities for cross regulation of these two developmentally important cell adhesion systems.

References

Aberle, H., H. Schwartz, and R. Kemler. 1996. Cadherin-catenin complex: protein interactions and their implications for cadherin function. *J. Cell. Biochem.* 61:514–523.

Balsamo, J., T.-C. Leung, H. Ernst, M.K.B. Zanin, S. Hoffman, and J. Lilien. 1996. Regulated binding of a PTP1B-like phosphatase to N-cadherin: control of cadherin-mediated adhesion by dephosphorylation of β-catenin. *J. Cell*

Biol. 134:801–813.

Balsamo, J., C. Arregui, T.C. Leung, and J. Lilien. 1998. The nonreceptor protein tyrosine phosphatase PTP1B binds to the cytoplasmic domain of N-cadherin and regulates the cadherin-actin linkage. *J. Cell Biol.* 143:523–532.

Bandyopadhyay, D., A. Kusari, K.A. Kenner, F. Liu, J. Chernoff, T.A. Gustafson, and J. Kusari. 1997. Protein-tyrosine phosphatase 1B complexes with the insulin receptor in vivo and is tyrosine-phosphorylated in the presence of insulin. *J. Biol. Chem.* 272:1639–1645.

Barry, S.T., and D.R. Critchley. 1994. The rho-dependent assembly of focal adhesions in Swiss 3T3 cells is associated with increased tyrosine phosphorylation and the recruitment of both pp125FAK and protein kinase C-γ to focal adhesions. *J. Cell Sci.* 107:2033–2045.

Behrens, J., L. Vakaet, R. Friis, E. Winterhager, F. Van Roy, M.M. Mareel, and W. Birchmeier. 1993. Loss of epithelial differentiation and gain of invasiveness correlates with tyrosine phosphorylation of the E-cadherin/β-catenin complex in cells transformed with a temperature-sensitive v-src gene. *J. Cell Biol.* 120:757–766.

Bergman, M., V. Joukov, I. Virtanen, and K. Alitalo. 1995. Overexpressed Csk tyrosine kinase is localized in focal adhesions, causes reorganization of αvβ5 integrin, and interferes with HeLa cell spreading. *Mol. Cell. Biol.* 15:711–722.

Black, D.S., and J.B. Bliska. 1997. Identification of p130Cas as a substrate of Yersinia YopH (Yop51), a bacterial protein tyrosine phosphatase that translocates into mammalian cells and targets focal adhesions. *EMBO (Eur. Mol. Biol. Organ.) J.* 16:2730–2744.

Bonnekoh, B., A. Wevers, F. Jugert, H. Merk, and G. Mahrle. 1989. Colorimetric growth assay for epidermal cell cultures by their crystal violet binding capacity. *Arch. Dermatol. Res.* 281:487–490.

Brown, M.T., and J.A. Cooper. 1996. Regulation, substrates and functions of Src. *Biochim. Biophys. Acta.* 1287:121–149.

Burridge, K., K. Fath, T. Kelly, G. Nuckolls, and C. Turner. 1988. Focal adhesions: transmembrane junctions between the extracellular matrix and the cytoskeleton. *Annu. Rev. Cell Biol.* 4:487–525.

Burridge, K., C.E. Turner, and L.H. Romer. 1992. Tyrosine phosphorylation of paxillin and pp125FAK accompanies cell adhesion to extracellular matrix: a role in cytoskeletal assembly. *J. Cell Biol.* 119:893–903.

Burridge, K., and M. Chrzanowska-Wodnicka. 1996. Focal adhesions, contractility and signaling. *Annu. Rev. Cell Biol.* 12:463–519.

Calalb, M.B., T.R. Polte, and S.K. Hanks. 1995. Tyrosine phosphorylation of focal adhesion kinase at sites in the catalytic domain regulates kinase activity: a role for Src family kinases. *Mol. Cell. Biol.* 15:954–963.

Clark, E.A., and J.S. Brugge. 1993. Redistribution of activated pp60c-src to integrin-dependent cytoskeletal complexes in thrombin-stimulated platelets. *Mol. Cell. Biol.* 13:1863–1871.

Clark, E.A., and J.S. Brugge. 1995. Integrins and signal transduction pathways: the road taken. *Science.* 268:233–239.

Cooper, J.A., and C.S. King. 1986. Dephosphorylation or antibody binding to the carboxy terminus stimulates pp60c-src. *Mol. Cell. Biol.* 6:4467–4477.

Courtneidge, S.A. 1985. Activation of the pp60c-src kinase by middle T antigen binding or by dephosphorylation. *EMBO (Eur. Mol. Biol. Organ.) J.* 4:1471–1477.

Daniel, J.M., and A.B. Reynolds. 1997. Tyrosine phosphorylation and cadherin/catenin function. *Bioessays.* 19:883–891.

Eide, B.L., C.W. Turck, and J.A. Escobedo. 1995. Identification of Tyr-397 as the primary site of tyrosine phosphorylation and pp60src association in the focal adhesion kinase, pp125. *Mol. Cell. Biol.* 15:2819–2827.

Ezumi, Y., H. Takayama, and M. Okuma. 1995. Differential regulation of protein-tyrosine phosphatases by integrin αIIbβ3 through cytoskeletal reorganization and tyrosine phosphorylation in human platelets. *J. Biol. Chem.* 270:11927–11934.

Fang, K.S., H. Sabe, H. Saito, and H. Hanafusa. 1994. Comparative study of three protein-tyrosine phosphatases. *J. Biol. Chem.* 269:20194–20200.

Flint, A.J., T. Tiganis, D. Bradford, and N. Tonks. 1997. Development of "substrate-trapping" mutants to identify physiological substrates of protein tyrosine phosphatases. *Proc. Natl. Acad. Sci. USA.* 94:1680–1685.

Frangioni, J.V., P.H. Beahm, V. Shifrin, C.A. Jost, and B.G. Neel. 1992. The nontransmembrane tyrosine phosphatase PTP-1B localizes to the endoplasmic reticulum via its 35 amino acid C-terminal sequence. *Cell.* 68:545–560.

Frangioni, J.V., A. Oda, M. Smith, E. Salzman, and B.G. Neel. 1993. Calpain-catalyzed cleavage and subcellular relocation of protein phosphotyrosine phosphatase 1B (PTP-1B) in human platelets. *EMBO (Eur. Mol. Biol. Organ.) J.* 12:4843–4856.

Fujii, K., F. Furukawa, and N. Matsuyoshi. 1996. Ligand activation of overexpressed epidermal growth factor receptor results in colony dissociation and disturbed E-cadherin function in HSC-1 human cutaneous squamous carcinoma cells. *Exp. Cell Res.* 223:50–62.

Giancotti, F.G., and E. Ruoslahti. 1990. Elevated levels of the α5β1 fibronectin receptor suppress the transformed phenotype of Chinese hamster ovary cells. *Cell.* 60:849–859.

Garton, A.J., M.R. Burnham, A.H. Bouton, and N.K. Tonks. 1997. Association of PTP-PEST with the SH3 domain of p130Cas; a novel mechanism of protein tyrosine phosphatase substrate recognition. *Oncogene.* 18:877–885.

Guan, J.-L., and D. Shalloway. 1992. Regulation of focal adhesion-associated protein kinase by both cellular adhesion and oncogenic transformation. *Nature.* 358:690–692.

Gumbiner, B.M. 1993. Proteins associated with the cytoplasmic surface of adhe-

sion molecules. *Neuron*. 11:551–564.

Hamaguchi, M., N. Matsuyoshi, Y. Ohnishi, B. Gotoh, M. Takeichi, and Y. Nagai. 1993. p60v-src causes tyrosine phosphorylation and inactivation of the N-cadherin-catenin cell adhesion system. *EMBO (Eur. Mol. Biol. Organ.) J.* 12:307–314.

Hanks, S.K., and T.R. Polte. 1997. Signaling through focal adhesion kinase. *Bioessays*. 19:137–144.

Hazan, R.B., and L. Norton. 1998. The epidermal growth factor receptor modulates the interaction of E-cadherin with the actin cytoskeleton. *J. Biol. Chem.* 273:9078–9084.

Hotchin, N.A., and A. Hall. 1995. The assembly of integrin complexes requires both extracellular matrix and intracellular rho/rac GTPases. *J. Cell Biol.* 131:1857–1865.

Howel, B.W., and J.A. Cooper. 1994. Csk suppression of Src involves movement of Csk to sites of Src activity. *Mol. Cell. Biol.* 14:5402–5411.

Ilic, D., Y. Furuta, S. Kanazawa, N. Takeda, K. Sobue, N. Nakatsuji, S. Nomura, J. Fujimoto, M. Okada, T. Yamamoto, and S. Aizawa. 1995. Reduced cell motility and enhanced focal adhesion contact formation in cells from FAK-deficient mice. *Nature*. 377:539–544.

Imamoto, A., and P. Soriano. 1993. Disruption of the cdk gene, encoding a negative regulator of src family tyrosine kinases, leads to neural tube defects and embryonic lethality in mice. *Cell*. 73:1117–1124.

Jockusch, B.M., P. Bubeck, K. Giehl, M. Kroemker, J. Moschner, M. Rothkegel, M. Rüdiger, K. Schlüter, G. Stanke, and J. Winkler. 1995. The molecular architecture of focal adhesions. *Annu. Rev. Cell Dev. Biol.* 11:379–416.

Jung, E.J., Y.-S. Kang, and C.W. Kim. 1998. Multiple phosphorylation of chicken protein tyrosine phosphatase 1 and human protein tyrosine phosphatase 1B by casein kinase II and p60$^{c\text{-}src}$ in vitro. *Biochem. Biophys. Res. Commun.* 246:238–242.

Kaplan, K.B., K.B. Bibbins, J.R. Swedlow, M. Arnaud, D.O. Morgan, and H.E. Varmus. 1994. Association of the amino-terminal half of c-Src with focal adhesions alters their properties and is regulated by phosphorylation of tyrosine 527. *EMBO (Eur. Mol. Biol. Organ.) J.* 13:4745–4756.

Kaplan, K.B., J.R. Swedlow, D.O. Morgan, and H.E. Varmus. 1995. c-Src enhances the spreading of src−/− fibroblasts on fibronectin by a kinase-independent mechanism. *Genes Dev.* 9:1505–1517.

Kemler, R. 1993. From cadherins to catenins: cytoplasmic protein interactions and regulation of cell adhesion. *Trends Genet.* 9:317–321.

Kenner, K.A., E. Anyanwu, J.M. Olefsky, and J. Kusari. 1996. Protein-tyrosine phosphatase 1B is a negative regulator of insulin- and insulin-like growth factor-1-stimulated signaling. *J. Biol. Chem.* 271:19810–19816.

Kornberg, L., H.S. Earp, J.T. Parsons, M. Schaller, and R.L. Juliano. 1992. Cell adhesion of integrin clustering increases phosphorylation of a focal adhesion associated tyrosine kinase. *J. Biol. Chem.* 267:23439–23442.

Krueger, J.G., E.A. Garber, and A.R. Goldberg. 1983. Subcellular localization of pp60src in RSV-transformed cells. *Curr. Top. Microbiol. Immunol.* 107:52–124.

Laemmli, U.K. 1970. Cleavage of structural proteins during the assembly of the head of bacteriophage T4. *Nature*. 227:680–685.

Lilien, J., S. Hoffman, C. Eisenberg, and J. Balsamo. 1997. β-Catenin is a target for extracellular signals controlling cadherin function: the neurocan-GalNAcPTase connection. *Curr. Top. Dev. Biol.* 35:161–189.

Lipfert, L., B. Haimovich, M.D. Schaller, B.S. Cobb, J.T. Parsons, and J.S. Brugge. 1992. Integrin-dependent phosphorylation and activation of the protein tyrosine kinase pp125FAK in platelets. *J. Cell Biol.* 119:905–912.

Liu, F., and J. Chernoff. 1997. Protein tyrosine phosphatase 1B interacts with and is tyrosine phosphorylated by the epidermal growth factor receptor. *Biochem. J.* 327:139–145.

Liu, F., D.E. Hill, and J. Chernoff. 1996. Direct binding of the proline-rich region of protein tyrosine phosphatase 1B to the Src homology 3 domain of p130(Cas). *J. Biol. Chem.* 271:31290–31295.

Liu, F., M.A. Sells, and J. Chernoff. 1998. Protein tyrosine phosphatase 1B negatively regulates integrin signaling. *Curr. Biol.* 8:173–176.

Luna, E.J., and A.L. Hitt. 1992. Cytoskeleton-plasma membrane interactions. *Science (Wash. DC)*. 258:955–964.

Machesky, L.M., and A. Hall. 1996. Rho: a connection between membrane receptor signalling and the cytoskeleton. *Trends Cell Biol.* 6:304–310.

Milarski, K.L., G. Zhu, C.G. Pearl, D.J. McNamara, E.M. Dobrusin, D. MacLean, A. Thieme-Sefler, Z.-Y. Zhang, T. Sawyer, S.J. Decker, et al. 1993. Sequence specificity in recognition of the epidermal growth factor receptor by protein tyrosine phosphatase 1B. *J. Biol. Chem.* 268:23634–23639.

Nada, S., M. Okada, A. MacAuley, J.A. Cooper, and H. Nakagawa. 1991. Cloning of a complementary DNA for a protein tyrosine kinase that specifically phosphorylates a negative regulatory site of p60c-src. *Nature*. 351:69–72.

Nada, S., T. Yagi, H. Takeda, T. Tokunaga, H. Nakagawa, Y. Ikawa, M. Okada, and S. Aizawa. 1993. Constitutive activation of Src family kinases in mouse embryos that lack CSK. *Cell*. 73:1125–1136.

Nermut, M.V., P. Eason, E.M.A. Hirst, and S. Kellie. 1991. Cell/substratum adhesions in RSV-transformed rat fibroblasts. *Exp. Cell Res.* 193:382–397.

Nigg, E.A., B.M. Sefton, T. Hunter, G. Walter, and S.J. Singer. 1982. Immunofluorescent localization of the transforming protein of Rous sarcoma virus with antibodies against a synthetic Src peptide. *Proc. Natl. Acad. Sci. USA*. 79:5322–5326.

Nobes, C.D., and A. Hall. 1995. Rho, rac, and cdc42 GTPases regulate the assembly of multimolecular focal complexes associated with actin stress fibers, lamellipodia, and filopodia. *Cell*. 81:53–62.

Okada, M., S. Nada, Y. Yamanishi, T. Yamamoto, and H. Nakagawa. 1991. CSK: a protein-tyrosine kinase involved in regulation of src family kinases. *J. Biol. Chem.* 266:24249–24252.

Ozawa, M., and R. Kemler. 1998. Altered cell adhesion activity by pervanadate due to the dissociation of α-catenin from the E-cadherin/catenin complex. *J. Biol. Chem.* 273:6166–6170.

Parsons, J.T. 1996. Integrin-mediated signalling: regulation by protein tyrosine kinases and small GTP-binding proteins. *Curr. Opin. Cell Biol.* 8:146–152.

Parsons, J.T., and S.J. Parsons. 1997. Src family protein tyrosine kinases: cooperating with growth factor and adhesion signaling pathways. *Curr. Opin. Cell Biol.* 9:187–192.

Ridley, A.J., and A. Hall. 1992. The small GTP-binding protein rho regulates the assembly of focal adhesions and actin stress fibers in response to growth factors. *Cell*. 70:389–399.

Rock, M.T., W.H. Brooks, and T.L. Rozman. 1997. Calcium-dependent signaling pathways in T cells. *J. Biol. Chem.* 272:33377–33383.

Rohrschneider, L.R. 1980. Adhesion plaques of Rous sarcoma virus-transformed cells contain the src gene product. *Proc. Natl. Acad. Sci. USA*. 77:3514–3518.

Schaller, M.D., and J.T. Parsons. 1995. pp125FAK-dependent tyrosine phosphorylation of paxillin creates a high-affinity binding site for Crk. *Mol. Cell Biol.* 15:2635–2645.

Schaller, M.D., J.D. Hildebrand, J.D. Shannon, J.W. Fox, R.R. Vines, and T. Parsons. 1994. Autophosphorylation of the focal adhesion kinase, pp125FAK, directs SH-dependent binding of pp60src. *Mol. Cell Biol.* 14:1680–1685.

Schwartz, M.A., M.D. Schaller, and M.H. Ginsberg. 1995. Integrins: emerging paradigms of signal transduction. *Annu. Rev. Cell Dev. Biol.* 11:549–599.

Seely, B.L., P.A. Staubs, D.R. Reichart, P. Berhanu, K.L. Milarski, A.R. Saltiel, J. Kusari, and J.M. Olefsky. 1996. Protein tyrosine phosphatase 1B interacts with the activated insulin receptor. *Diabetes*. 45:1379–1385.

Seufferlein, T., and E. Rozengurt. 1994. Lysophosphatidic acid stimulates tyrosine phosphorylation of focal adhesion kinase, paxillin and p130. *J. Biol. Chem.* 269:9345–9351.

Shen, Y., G. Schneider, J.-F. Cloutier, A. Veillete, and M.D. Schaller. 1998. Direct association of protein-tyrosine phosphatase PTP-PEST with paxillin. *J. Biol. Chem.* 273:6474–6481.

Soltesz, S.A., E.A. Powers, J.G. Geng, and C. Fisher. 1997. Adhesion of HT-29 colon carcinoma cells to E-selectin results in increased tyrosine phosphorylation and decreased activity of c-src. *Int. J. Cancer*. 71:645–653.

Somani, A.-K., J.S. Bignon, G.B. Mills, K.A. Siminovitch, and D.R. Branch. 1997. Src kinase activity is regulated by the SHP-1 protein-tyrosine phosphatase. *J. Biol. Chem.* 272:21113–21119.

Soriano, P., C. Montgomery, R. Geske, and A. Bradley. 1991. Targeted disruption of the c-src proto-oncogene leads to osteopetrosis in mice. *Cell*. 64:693–702.

Takeya, T., and H. Hanafusa. 1983. Structure and sequence of the cellular gene homologous to the RSV src gene and the mechanism for generating the transforming virus. *Cell*. 32:881–890.

Tamura, M., J. Gu, K. Matsumoto, S.A. Aota, R. Parsons, and K.M. Yamada. 1998. Inhibition of cell migration, spreading, and focal adhesions by tumor suppressor PTEN. *Science*. 280:1614–1617.

Terasaki, M., and T.S. Reese. 1992. Characterization of endoplasmic reticulum by co-localization of BiP and dicarbocyanine dyes. *J. Cell Sci.* 101:315–322.

Thomas, S.M., P. Soriano, and A. Imamoto. 1995. Specific and redundant roles of Src and Fyn in organizing the cytoskeleton. *Nature*. 376:267–271.

Woodford-Thomas, T.A., J.D. Rhodes, and J.E. Dixon. 1992. Expression of a protein tyrosine phosphatase in normal and v-src–transformed mouse 3T3 fibroblasts. *J. Cell Biol.* 117:401–414.

Xing, Z., H.C. Chen, J.K. Nowlen, S.L. Taylor, D. Shalloway, and J.L. Guan. 1994. Direct interaction of v-Src with the focal adhesion kinase mediated by the Src SH2 domain. *Mol. Biol. Cell*. 5:413–421.

Yamada, K.M. 1997. Integrin signaling. *Matrix Biol.* 16:137–141.

Yamada, K.M., and B. Geiger. 1997. Molecular interactions in cell adhesion complexes. *Curr. Opin. Cell Biol.* 9:76–85.

Zachary, I., J. Sinnet-Smith, C.E. Turner, and E. Rozengurt. 1993. Bombesin, vasopresin and endothelin rapidly stimulate tyrosine phosphorylation of the focal adhesion associated protein paxillin in Swiss 3T3 cells. *J. Biol. Chem.* 268:22060–22065.